Full-scale flexural testing of slabs made of modular structural concrete insulated panels

Mahesh Acharya, Karma Gurung, and Mustafa Mashal

- This study presents a novel type of structural concrete insulated panel that can be fabricated with modular, off-the-shelf components for use in residential homes and low-rise structures.
- Benefits of this structural concrete insulated panel include time savings during construction, lightweight members, and using recycled components. This technology allows for fabrication on-site, which is beneficial for reconstruction needs in areas affected by natural disasters.
- Full-scale test specimens were fabricated and tested to investigate flexural behavior, strength, ductility, and failure mechanisms. The test program included three short-span specimens, three medium-span specimens, and five long-span specimens. Of the long-span specimens, two were fabricated with additional reinforcement in the splice region.

The structural concrete insulated panel (SCIP) technique was initially called "thin-shell sandwich panel" construction. It was developed in the late 1960s by Victor Weismann in Pasadena, Calif.[1] SCIPs are used as slab and wall systems in a variety of structures. They can be considered for fast and economical construction of low-rise buildings. In this study, a novel precast concrete approach for modular SCIPs is proposed for use in residential homes and low-rise structures.

Background

A typical SCIP is composed of an insulated core made of expanded polystyrene (EPS) foam flanked on both sides by galvanized steel wire mesh, with the two sides of mesh held together using diagonal steel shear connectors. A layer of concrete is applied on each side of the panel to provide structural resistance. The concrete layer is generally 1 to 2 in. (25.4 to 50 mm) thick and has a 28-day compressive strength of 3000 to 4000 psi (20 to 28 MPa). Over the years, many versions of SCIPs have been developed by various manufacturers around the world. **Figure 1** shows the details of a SCIP produced in the United States by producer A.

A typical SCIP manufactured by producer A uses modular, off-the-shelf materials that are readily available. The key elements consist of a recycled EPS core, cold-rolled galvanized steel mesh, and a diagonal truss connector. The panels use Type I EPS that complies with ASTM C5782 for

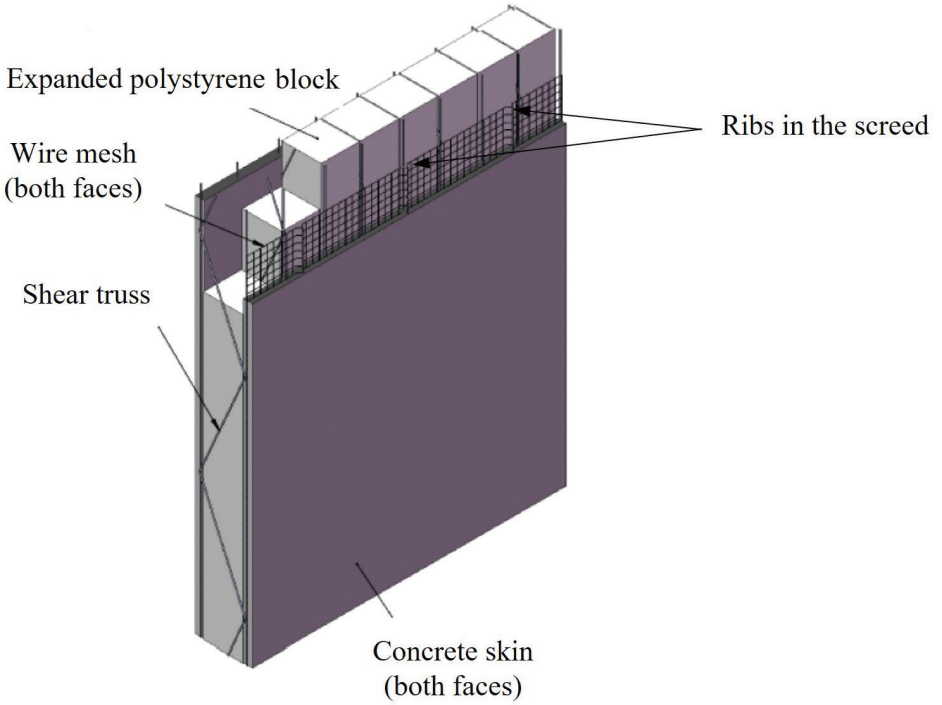

Figure 1. Details of a structural concrete insulated panel from producer A in the United States. Note: EPS = expanded polystyrene.

the insulation core (**Fig. 2**). The core has a maximum density of 1.0 lb/ft^3 (16 kg/m^3) and a modulus of elasticity of 180 to 220 psi (1.24 to 1.52 MPa). The blocks of EPS used to produce the panels are generally 6 in. (152 mm) wide and 10 ft (3 m) long and have a varying thickness of 3 to 11 in. (76 to 280 mm). Two EPS blocks can be combined to produce panels longer than 10 ft.

The EPS core is flanked on both sides using a 1 by 1 in. (25.4 by 25.4 mm), cold-rolled, 14 gauge (1.63 mm) galvanized wire mesh. The mesh complies with the ASTM A1064[3] standard. The wire mesh has a screed system installed, which allows for easy application of concrete. To ensure that a uniform layer of concrete is applied on the panels, the wire mesh has two screed ribs 12 in. (300 mm) off center on both

Expanded polystyrene blocks

Diagonal shear connectors and trusses

Figure 2. Off-the-shelf components of structural concrete insulated panels from producer A.

sides (Fig. 1). A spacing of 0.5 in. (12.5 mm) is maintained between the EPS and the mesh to ensure that the mesh achieves sufficient concrete embedment and cover.

The two layers of mesh are held together using a 3⁄16 in. (4.76 mm) galvanized steel wire truss (Fig. 2), commonly referred to as shear connectors. The truss connectors meet ASTM A951,[4] ASTM A1064,[3] and ASTM A641[5] specifications. These truss connectors are typically used in the horizontal mortar joints for masonry walls to provide enhanced shear resistance. In the panel shown in Fig. 1, the diagonal bars transfer the longitudinal shear stress in between the two load-bearing faces. The shear trusses are spaced every 6 in. (152 mm) and are sandwiched in between the two EPS blocks. They are tied to the mesh using a pneumatic hog ring tie. There is a tolerance for a mesh of ¼ in. (6.35 mm) overall. The trusses are a standard size, and they help maintain a uniform distance between the mesh because the height of the truss is essentially equal to the width of the core.

A portable hydraulic jig press is used to assemble the EPS, steel mesh, and truss to produce a SCIP core. The portable jig press in this study has the capacity to produce panels that are 2 to 4 ft (0.6 to 1.2 m) wide, 10 to 18 ft (3 to 5.5 m) long, and 6 to 13 in. (150 to 330 mm) thick.

There have been many applications of SCIPs produced by various manufacturers for residential and military buildings in Europe, the Middle East, New Zealand, the United States, and elsewhere. **Figure 3** shows a typical construction sequence using SCIPs. The shotcrete has a 28-day compressive strength of 3000 to 4000 psi (20 to 28 MPa) for on-site application. The concrete layers could be applied either by hand or by using the shotcrete technology, which can be either a dry or wet process, depending on the application and availability of local resources and equipment. In a dry-mix process, the dry cementitious mixture is blown through a hose to the nozzle and water is injected immediately. In a wet-mix process, the ready-mixed concrete is pumped to the nozzle and compressed air is introduced at the nozzle to impel the mixture onto the receiving surface. Generally, a dry application is preferred. When a dry application is used, the water and prebagged shotcrete material are mixed at the nozzle before the mixture is sprayed.

SCIPs offer many advantages, such as faster construction, more-lightweight members (due to the lack of a solid core), superior quality, good thermal insulation, enhanced sound insulation, recycled components (for example, EPS blocks), and reduced environmental impact. In addition, the reduction in construction time, building equipment, concrete formwork, and skilled labor results in an economical and cost-effective alternative for low-rise residential structures as well as other structures. SCIPs can be combined with traditional concrete or steel frames for certain structures subjected to higher gravity or lateral loads.

Previous research

Although there have been numerous applications of SCIP technology in the past,[6] SCIPs have not been extensively investigated by researchers. Following is a brief review of the limited number of experimental and analytical studies available on the performance of SCIPs.

Kabir[7] investigated the flexural and shear loading on bearing walls and floor slabs made of SCIPs. The research presented load-deflection plots and the failure mechanism for SCIPs. The research concluded that in the linear elastic zone, basic equations from reinforced concrete mechanics can be applied to predict the stresses and strength of the panels.

Matz et al.[8] presented structural design and detailing considerations for buildings made of SCIPs. Kabir et al.[9] studied the nonlinear seismic response of steel frames with SCIP infills and demonstrated that such a system can be feasible in seismic zones.

Fouad et al.[10] conducted experimental testing of full-scale slab and wall panels under gravity loads. The specimens lacked proper detailing and edge constraints, which led to premature shear failure under flexural testing. The researchers proposed some analytical methods for estimating the flexural strength of the panels.

Rezaifar et al.[11] conducted shake table testing to investigate the dynamic behavior of a full-scale single-story structure built with SCIPs. In another study, Rezaifar et al.[12] conducted shake table testing of a scaled four-story building with SCIPs. Both studies showed considerable resistance of SCIPs during high-level earthquake vibrations.

Mashal[6] and Mashal and Filiatrault[1] used extensive nonlinear static and dynamic analyses to quantify the seismic performance factors for SCIPs. Their research concluded that SCIPs have great resistance and potential for use in seismic zones.

El Demerdash[13] carried out full-scale monotonic and cyclic testing of slabs and walls made of SCIPs with different concrete applications (for example, hand-applied versus pneumatically applied methods). The research also presented analytical finite element modeling for predicting the behavior of SCIPs under various loading scenarios.

Joseph et al.[14] studied the flexural behavior of SCIPs under punching and bending. This study found that such loading can significantly alter the behavior of SCIPs.

Gurung[15] conducted full-scale testing of modular SCIPs. This research introduced precasting technology for SCIPs and presented analytical equations and detailing considerations for buildings located in seismic and nonseismic regions.

Figure 3. Typical construction sequence for a residential house using structural concrete insulated panels.
Note: SCIP = structural concrete insulated panel.

Study objectives

Among several types of SCIPs manufactured around the world, this study is focused on the SCIPs manufactured by producer A (Fig. 1) in the United States. This particular panel is a modular version of a SCIP in the sense that off-the-shelf materials are used to produce the cores. Conventional SCIPs are fabricated in a production plant with sophisticated processes for welding and connecting the trusses and side mesh. The modular technology allows fabrication of the panels on-site, without the need for a production facility. This is important for reconstruction efforts in areas affected by natural hazards such as earthquakes and hurricanes. The SCIPs from producer A in this study can be made on-site or transported as individual components, depending on the location and availability of resources. The individual components could be assembled into panels using a portable hydraulic jig press and pneumatic hog rings.

SCIPs are not limited to resisting gravity loads; they can also be used as shear walls.

Mashal et al.[16] carried out full-scale testing of cantilever SCIPs under in-plane quasi-static cyclic loading. The wall-to-footing connection was a socket connection (**Fig. 4**). The specimens showed ductile behavior under lateral loads. Figure 4 presents a concept for the slab-to-wall connection where the joint between the panels is spliced to emulate monolithic construction and behavior. The connection features an L mesh and no. 3 (10M) hairpins, which can be designed and detailed similar to a wall-to-slab connection for a monolithic structure.

There are very limited experimental data available for modular SCIPs. Following are the objectives of this research:

- demonstrate a novel precast concrete approach for construction of SCIPs
- present detailing considerations to enhance the performance of SCIPs under flexural loading
- experimentally test full-scale SCIPs under the four-point bending test
- identify relevant failure mechanisms for modular SCIPs under flexural loading
- propose an adequate splicing detail for modular SCIPs with spans longer than 10 ft (3 m)
- compare the strength and deflection of modular SCIPs against requirements from U.S. building codes
- quantify the composite action for modular SCIPs

Description of test specimens

The novel precast concrete approach for modular SCIPs proposed in this study uses technology that is similar to tilt-up construction, which is common in the precast concrete industry for the construction of sandwich wall and slab panels. Precast concrete technology allows for the user to take full advantage of faster construction for SCIPs. It improves the final quality of the panels, accelerates construction, and eliminates the need to spray concrete on-site. In addition, it reduces the on-site labor and equipment costs. This study considered two sets of specimens for experimental testing: SCIPs without additional splice reinforcement and SCIPs with additional splice reinforcement. These sets are described further in the following sections.

The test specimens in this research were 4 ft (1.2 m) wide, 6 in. (152 mm) thick, and 10 to 18 ft (3 to 5.5 m) long. For each specimen, the EPS blocks were 6 in. wide, 4 in. (100 mm) thick, and 10 ft long. The 14-gauge (1.63 mm) wire mesh used on both sides of the EPS blocks was spaced 1 in. (25.4 mm) apart in both the transverse and longitudinal directions. The shear trusses were $\frac{3}{16}$ in. (4.7 mm) in diameter and spaced 6 in. apart. The concrete layer on each side was selected to be 1 in. thick; however, the concrete skin thickness could be greater than 1 in. based on the total thickness of panel. Experimental

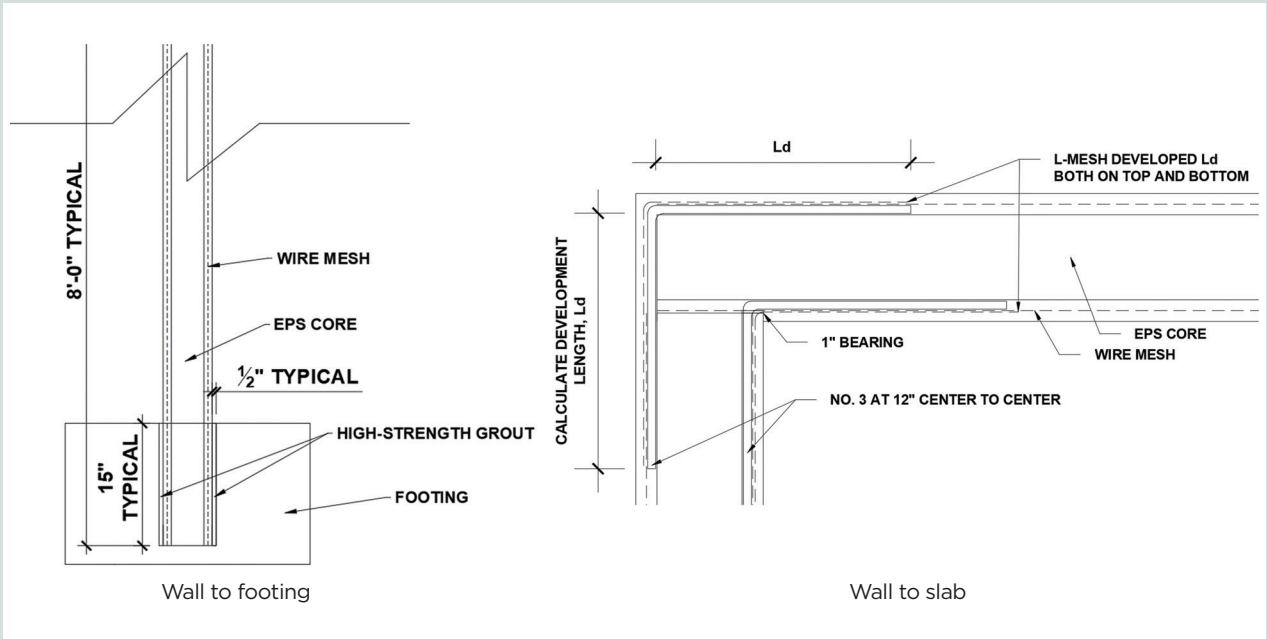

Figure 4. Typical connection detail for structural concrete insulated panels. Note: EPS = expanded polystyrene. No. 3 = 10M; 1" = 1 in. = 25.4 mm; 1' = 1 ft = 0.305 m.

studies on other types of SCIPs by El Demirdash[13] used thicker concrete skins (for example, 1.75 in. [44.5 mm]).

SCIPs without additional splice reinforcement

In the first set of specimens, three different spans were selected to study the out-of-plane flexural behavior of modular SCIPs. The three different spans were classified as short span, medium span, and long span, with lengths of 10, 14, and 18 ft (3, 4.3, and 5.5 m), respectively. For each span, three identical specimens were produced. The short-span specimens were labeled A-1, A-2, and A-3; the medium-span specimens were labeled B-1, B-2, and B-3; and the long-span specimens were labeled C-1, C-2, and C-3. **Table 1** presents the testing matrix for specimens without additional reinforcement.

Given their shorter length, the short-span SCIP cores did not have to be spliced; however, the medium- and long-span cores were spliced using flat mesh on each side of the panel and the EPS blocks were staggered (**Fig. 5**). This is a typical splicing detail for SCIPs; however, there is limited experimental work available to validate the adequacy of the splice with mesh without additional reinforcing bars. The splice mesh used in this set of specimens was similar to the mesh used on the skins of the SCIP core.

Table 1. Testing matrix for structural concrete insulated panels without additional splice reinforcement

Span length	Specimens	Dimensions, in.	Clear span, ft
Short	A-1, A-2, A-3	123 × 49 × 6	10
Medium	B-1, B-2, B-3	171 × 49 × 6	14
Long	C-1, C-2, C-3	219 × 49 × 6	18

Note: 1 in. = 25.4 mm; 1 ft = 0.305 m.

Figure 6 illustrates a typical cross section of the specimens used in this study. The edges of the panels were confined to

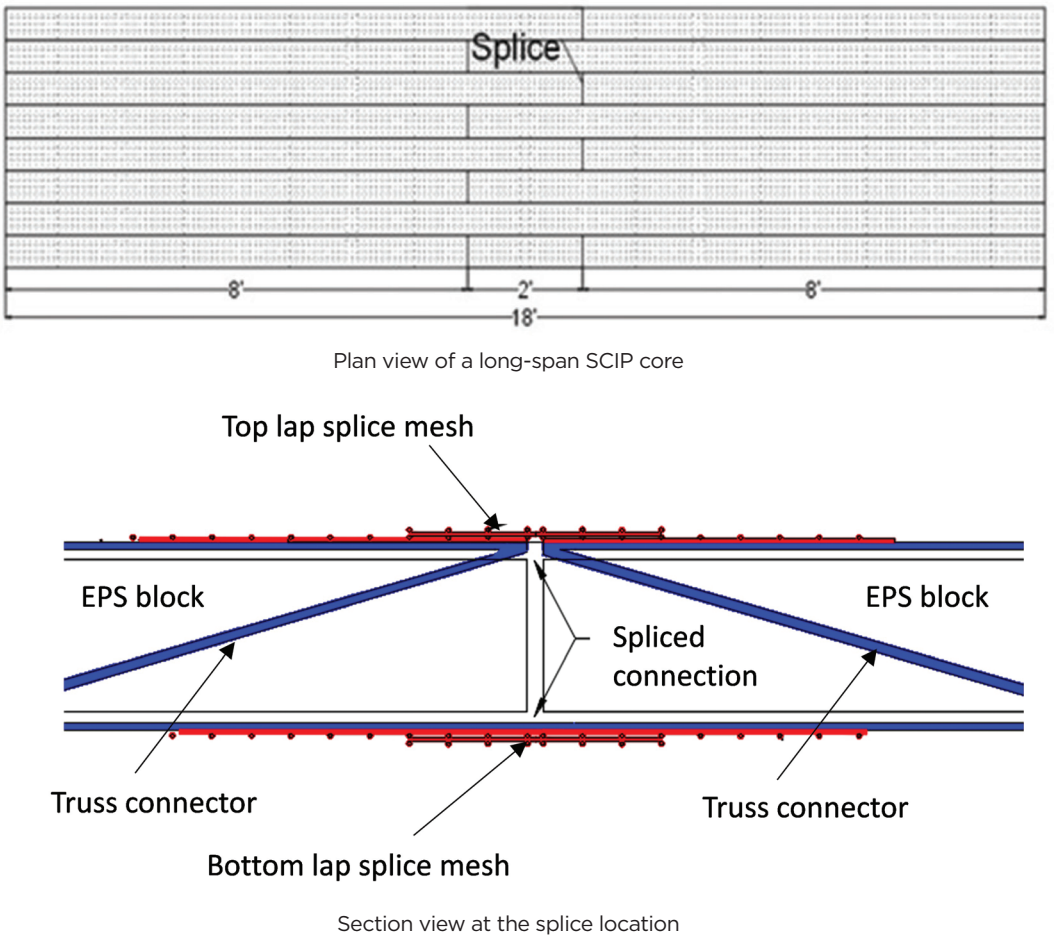

Plan view of a long-span SCIP core

Section view at the splice location

Figure 5. Typical splice detail without additional reinforcing bars. Note: EPS = expanded polystyrene; SCIP = structural concrete insulated panel. 1' = 1 ft = 0.305 m.

avoid premature failure caused by out-of-plane buckling of the diagonal bars, which was first observed by Fouad et al.[10] This is a detailing consideration meant to enhance structural performance. The edges of the panel were confined using a U mesh along with a 0.5 in. (12.5 mm) thick concrete skin (**Fig. 7**). The U mesh was identical to the wire mesh used on each side of the core.

SCIPs with additional splice reinforcement

Two additional long-span specimens were produced for testing. These specimens incorporated additional reinforcement of Grade 60 (413 MPa), no. 3 (10M) reinforcing bars in the splice region. These specimens are referred to as modified long spans (**Table 2**). The modified long-span specimens were labeled S-1 and S-2.

The ultimate moment capacity of the short-span specimen was used to determine the amount of additional reinforcement required to provide an adequate splice. Panels were assumed to have a fully composite section to determine the amount of additional reinforcement required. The reinforcing bars were extended as required to achieve full development length as required by the American Concrete Institute's *Building Code Requirements for Structural Concrete (ACI 318-19) and Com-*

Table 2. Testing matrix for structural concrete insulated panels with additional splice reinforcement

Span length	Specimens	Dimensions, in.	Clear span, ft
Long	S-1, S-2	219 × 49 × 6	18

Note: 1 in. = 25.4 mm; 1 ft = 0.305 m.

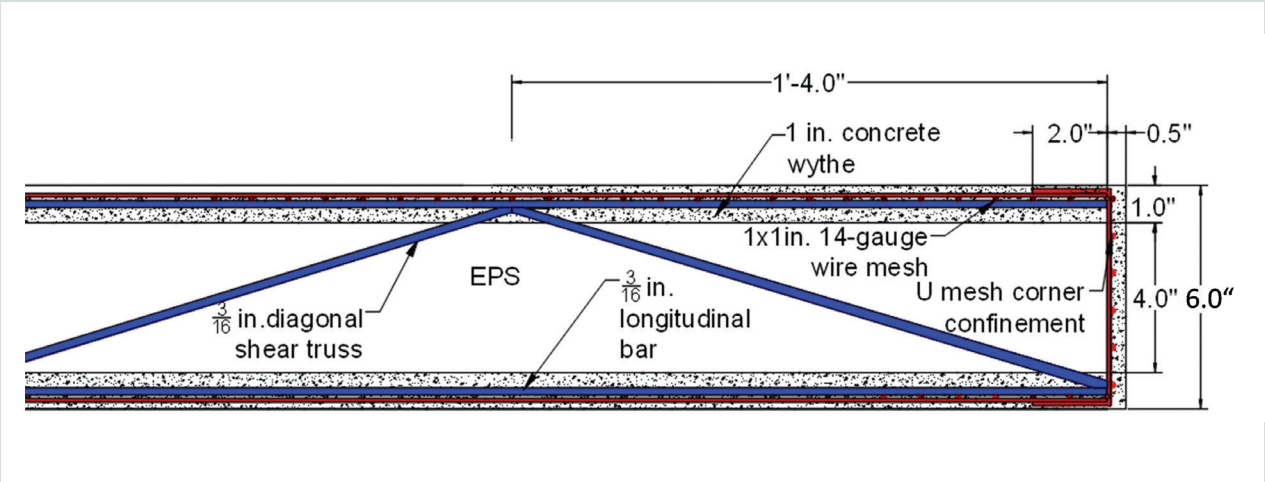

Figure 6. Cross section of a typical slab specimen. Note: 1" = 1 in. = 25.4 mm; 1' = 1 ft = 0.305 m.

Figure 7. Modular structural concrete insulated panel cores without additional reinforcement in the splice zones.

mentary (ACI 318R-19)[17] to avoid pullout failure. **Figure 8** presents the splice details for the modified long spans.

For the additional reinforcing bars in the splice region, two configurations were explored. For the preparation of S-1, seven Grade 60 (413 MPa), no. 3 (10M) bars were used at 8 in. (203.2 mm) center to center (**Fig. 9**). The bars were tied in between the mesh and the EPS core. For S-2, nine Grade 60, no. 3 bars were used at 6 in. (152 mm) center to center, placed in a staggered orientation (Fig. 9). Similar to S-1, the bars were tied between the mesh and the EPS core.

Concrete mixture design and construction technology

Instead of using the traditional shotcrete process, we used an alternative precast concrete approach to prepare the specimens. A self-consolidating concrete (SCC) with a high-strength mixture

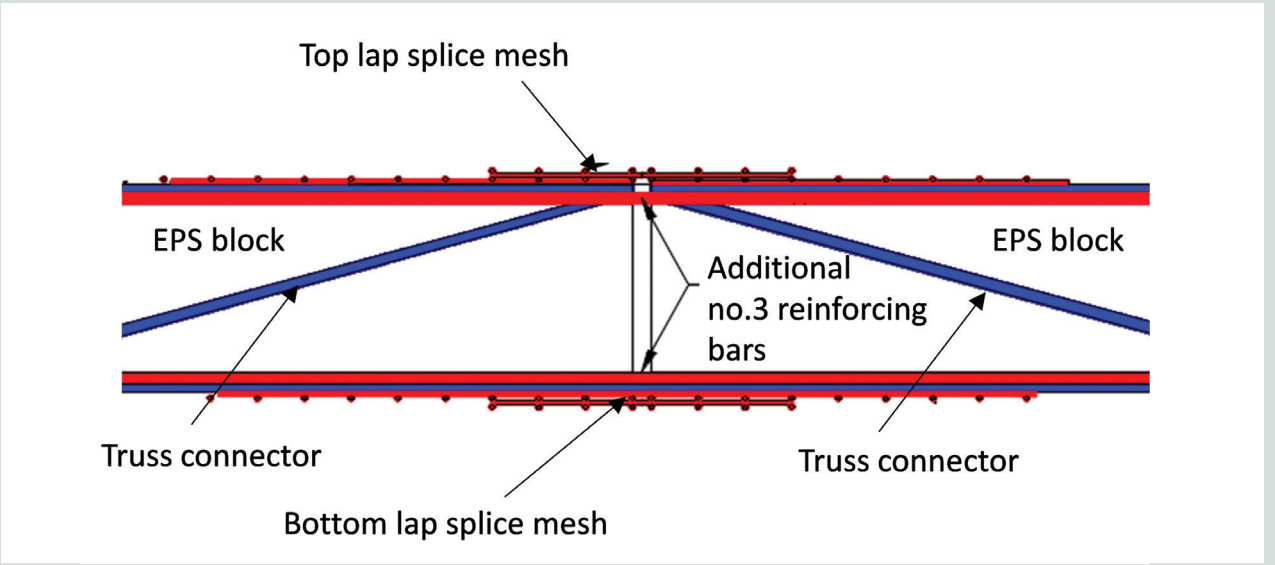

Figure 8. Typical splice detail with additional reinforcing bars. Note: EPS = expanded polystyrene. No. 3 = 10M.

Specimen S-1

Specimen S-2

Figure 9. Modular structural concrete insulated panel cores with additional reinforcement in the splice zones.

was used for the concrete wythes, with a target compressive strength of at least 6000 psi (41 MPa). This compressive strength is consistent with what was used for the production of tilt-up panels in the precast concrete industry. The ACI 211.1[18] absolute volumetric method was used to design and produce the SCC mixture (**Table 3**). A high-range water-reducing admixture was used to achieve high workability for the concrete mixture without compromising compressive strength.

The SCC mixture was designed to have an average spread of 23.5 in. (597 mm). Other properties of the SCC mixture considered in this research are listed in **Table 4**.

For construction of the specimens, a precasting bed was prepared. Because the span of the specimens varied, the walls of the precasting bed were made modular using 0.75 in. (19 mm) thick plywood and 1.5 by 3.5 in. (38 by 89 mm) Douglas fir lumber. Plastic liner was applied to extend the life of the bed, avoid concrete leakage, and provide a smooth finish.

Once the precasting bed was ready for the concrete to be placed, the materials used to make the SCC mixture were batched in buckets and then mixed using a 3.5 ft^3 (0.1 m^3) concrete mixer. For typical construction of a specimen, the concrete layer was applied on the SCIP core in two lifts. First, the bottom layer of concrete was placed and spread on the bed until a 1 in. (25.4 mm) thick uniform layer was obtained.

Table 3. Self-consolidating concrete mixture proportions

Item	Amount
Cement	729.0 lb/yd^3
Fly ash	183.2 lb/yd^3
Coarse sand	1701.0 lb/yd^3
Fine pea gravel	810.0 lb/yd^3
Water	364.5 lb/yd^3
High-range water reducing admixture	10.4 oz/100 lb

Note: 1 oz = 29.57 mL; 1 lb = 0.454 kg; 1 lb/yd^3 = 0.59 kg/m^3.

Table 4. Self-consolidating concrete mixture properties

Parameters	Targeted values
Spread	23.5 in.
Air content	4.5%
Water-cement ratio	0.40
Fine aggregate-to-coarse aggregate ratio	0.25
Unit weight	144.7 lb/ft^3

Note: 1 in. = 25.4 mm; 1 lb/yd^3 = 0.59 kg/m^3.

After this uniform bottom layer was obtained, the fabricated panel was placed on top of the concrete layer. It was important to make sure that the panel was placed properly inside the precasting bed to maintain the required cover concrete on each side. The top layer of concrete was placed without any delays, and then the concrete surface was finished. The screed rib, placed in the mesh as a guide, was used to provide a uniform 1 in. (25.4 mm) thick top layer of concrete cover.

A plastic liner was used to cover the concrete. The specimen was then cured inside the bed using burlap for at least three days before being taken out of the bed. The specimen was taken out of the formwork by removing the modular walls in the formwork, and then the specimen was transported to the moist curing rack until it was ready for testing at 28 days. The specimen was lifted and transported on its side using a spreader steel beam and construction-grade straps. After the specimen was fully cured, it was painted white to enhance the visibility of cracks during testing and to clearly mark the cracks that occurred.

Material characterization

Tensile testing of samples was performed for the mesh and the truss. The testing was in accordance with ASTM E8.[19] There were three samples tested from each component (mesh and truss). The average ultimate strength was 81.9 ksi (565 MPa) for the 3⁄16 in. (4.76 mm) truss and 70.3 ksi (485 MPa) for the 14-gauge (1.63 mm) wire mesh.

The concrete compressive strength varied from 4290 psi (30 MPa) at 3 days to 8491 psi (59 MPa) at 28 days. All of the concrete specimens were tested in accordance with ASTM C39[20] and ASTM C496.[21]

Testing arrangement

Testing included four-point bending tests in accordance with the guidelines provided in ASTM E72.[22] The four-point bending test corresponded to transverse out-of-plane loading of the slab panels. **Figure 10** illustrates the four-point bending test setup.

The specimens were oriented horizontally and seated on a stiff steel beam using a 1 in. (25.4 mm) roller. In addition, a ½ in. (12.75 mm) thick steel plate with rubber padding was installed between the specimen and the roller support across its entire width to avoid bearing failure. The roller did not wobble or bend during the testing. **Figure 11** presents details of the support for the specimens. The vertical load was applied to the slab panels by using two-point loads at one-quarter of the span of the specimen. The two-point loads were created by pushing down on a spreader beam with a servo-valve actuator. The spreader beam was seated on a 2 in. (50.8 mm) roller and ¾ in. (19 mm) thick steel plate with rubber padding (Fig. 11).

A monotonic quasi-static loading protocol was used to test the specimen. The loading protocol was slow testing with negligible inertial dynamic effects, as outlined in ASTM E72.[22] The transverse out-of-plane loading was applied to the specimen by a deflection-controlled servo-hydraulic actuator. The loading rate was set at 0.04 in./sec (1 mm/sec) applied at an increment of 500 lb (2224 N) and continued until failure. At each load increment, the maximum load was held constant for a certain amount of time to mark the cracks and observe the cracking pattern and propagation. The load was then released slowly, which allowed the specimen to stabilize and be prepared for another load increment. The midpoint deflections of the specimen were measured using string potentiometers, which were installed on the adjacent edges of the centerline of the specimen. The data acquisition system recorded the loads and deflections at the rate of one data point per second.

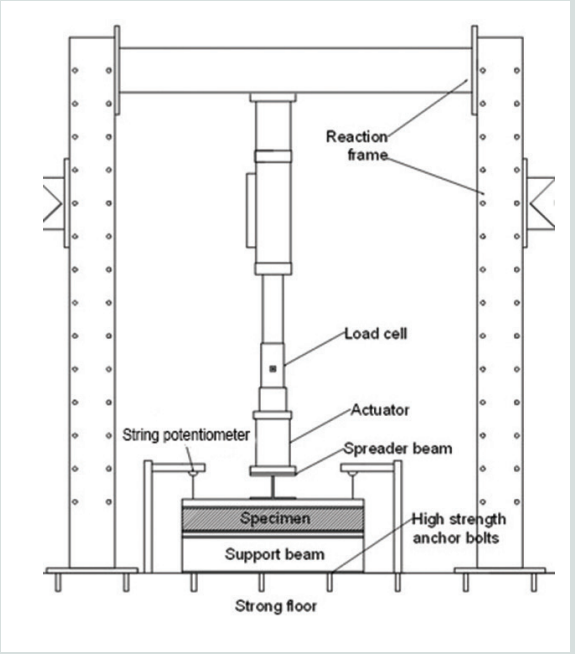

Figure 10. Experimental setup for the four-point bending test.

Experimental testing

Short-span specimens

Three short-span slabs—A-1, A-2, and A-3—were tested (Table 1). The specimens were 123 in. (3124 mm) long by 49 in. (1245 mm) wide by 6 in. (152 mm) thick. The short-span slabs had a simply supported span of 119 in. (3023 mm). **Figure 12** presents the schematic details and the test setup for the short-span slab specimens.

During the load level of 6.5 and 7 kip (29 and 31 kN), hairline cracks (less than 0.016 in. [0.4 mm] in width) appeared on the bottom wythe in all specimens between the point loads (critical moment region). This can be observed in the load-deflection plot of **Fig. 13** as a slight bend in the curves. As the load increased, the cracks became wider and longer. Simultaneously, more cracks appeared inside the critical moment region until a dominant crack was formed. Fewer cracks were observed outside the critical moment region as the load was increased incrementally. The dominant crack extended throughout the width of the panel, which marked the failure plane. The number of flexural cracks that were appearing on the bottom wythe signified that the specimens were able to redistribute the stresses and achieve a good level of ductility.

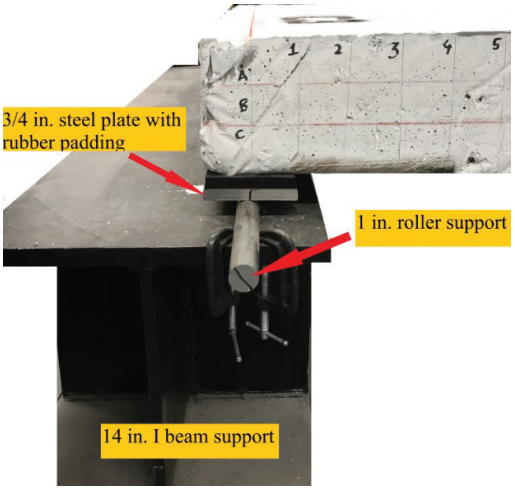

End support

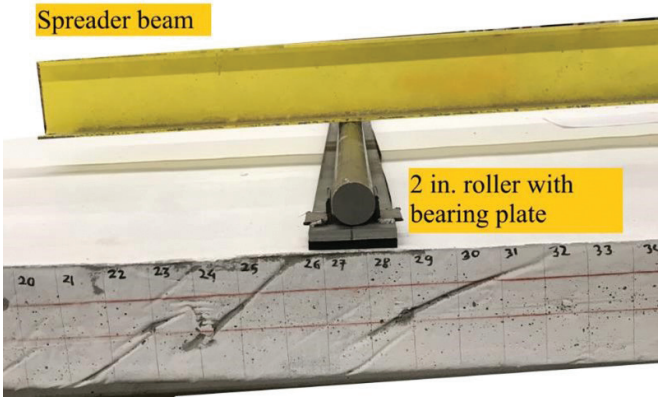

Load application point

Figure 11. Testing setup details. Note: 1 in. = 25.4 mm.

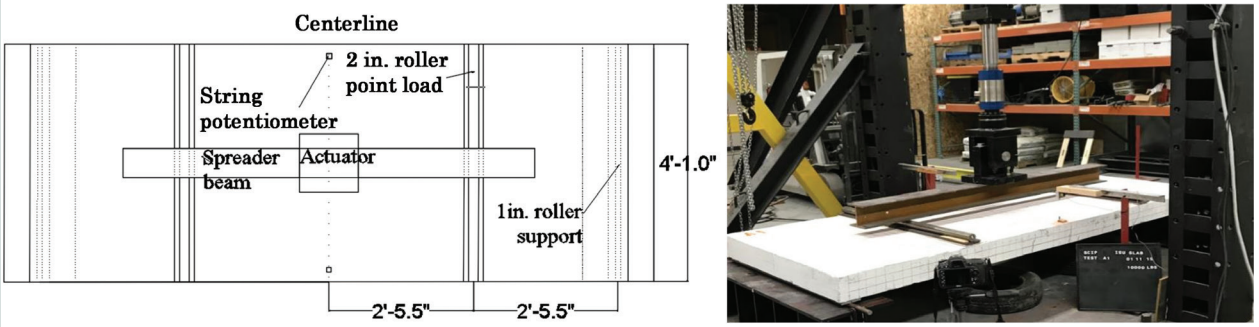

Figure 12. Experimental test setup of the short-span specimens. Note: 1" = 1 in. = 25.4 mm; 1' = 1 ft = 0.305 m.

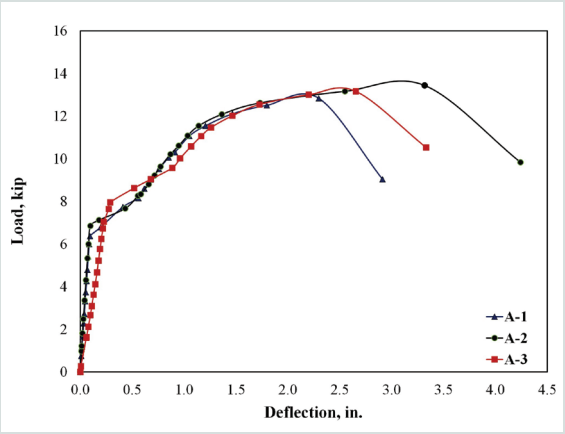

Figure 13. Load-deflection curves for the short-span specimens A-1, A-2, and A-3. Note: A-1 = specimen A-1; A-2 = specimen A-2; A-3 = specimen A-3. 1 in. = 25.4 mm; 1 kip = 4.448 kN.

The mode of failure for all short-span specimens was ductile, dominated by flexural action. The panels exhibited significant inelastic deformation prior to failure.

Failure occurred inside the critical moment region, but it was not exactly at the center of the panel. The failure planes for A-1 and A-3 were located 12.5 and 13.5 in. (320 and 343 mm) above the centerline, respectively. For A-2, the failure plane was 12.8 in. (325 mm) below the centerline. Small and large popping sounds were heard throughout the testing. These sounds correlated with the snapping of the mesh and the chords for the trusses. **Figure 14** shows observed failure mechanisms from testing the short-span specimens. **Table 5** summarizes the capacities from testing the short-span specimens.

Medium-span specimens

The medium-span slab specimens—B-1, B-2, and B-3—were 171 in. (4343 mm) long by 49 in. (1245 mm) wide by 6 in. (152 mm) thick and had a simply supported span of 167 in.

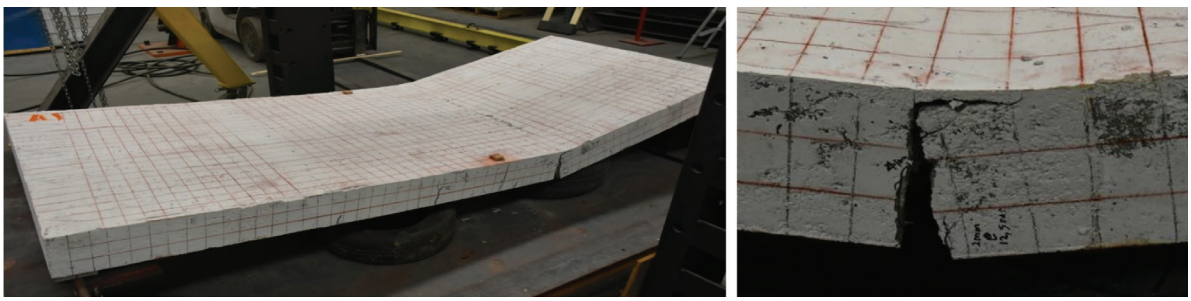

Figure 14. Failure modes for short-span specimen A-1.

Table 5. Summary of test results for short-span specimens

Specimen	f'_c, psi	k, lb/in.	M_{cr}, kip-ft	M_{max}, kip-ft	δ, in.	W, lb/ft²
A-1	8657	68,475	7893	15,914	2.30	317.0
A-2	8346	70,329	8495	16,659	3.32	331.9
A-3	8732	37,046	7715	16,320	2.65	325.0
Average	8578	58,617	8034	16,297	2.76	325

Note: f'_c = compressive strength of concrete at 28 days; k = elastic stiffness; M_{cr} = cracking moment; M_{max} = ultimate moment capacity; W = ultimate uniform load that can produce a similar ultimate moment capacity M_{max}; δ = deflection at ultimate load. 1 in. = 25.4 mm; 1 lb/in. = 0.00018 kN/mm; 1 kip-ft = 1.356 kN-m; 1 psi = 6.895 kPa; 1 lb/ft² =4.88 kg/m².

(4242 mm). **Figure 15** presents the schematic details and the test setup for the medium-span slab specimens.

Unlike the short-span specimens that were fabricated using continuous sections of EPS, mesh, and diagonal trusses, the medium-span specimens had a splice that was located at the center of the panels. Because all of the components used to fabricate the panels came in 10 ft (3 m) sections, two pieces were formed in the middle of the panel. A typical splice reinforcement technique of overlapping the mesh at the splice region was used. The two splice planes, labeled A and B, can be seen in the schematic presented in Fig. 15.

Hairline cracks appeared on the bottom wythe in the critical moment region during load levels of 2 and 2.5 kip (8.9 and 11.1 kN). After the formation of the first crack, the specimen yielded shortly thereafter and did not return to its original position after the applied load was removed. As the load was increased, a dominant crack appeared in the splice region and continually became wider and longer during testing. Compared with the short-span specimens, the medium-span slabs had fewer flexural cracks throughout testing.

The mode of failure for all three medium-span specimens was sudden premature failure at the splice location before the true capacity of the panel was reached (**Fig. 16**). The premature failure was caused by insufficient flexural capacity at the splice location. This caused the specimens to show a relatively low range of inelastic behavior under flexural loading. Observation from testing indicated some degree of stress redistribution in the medium-span specimens; however, few cracks appeared outside of the critical moment region as the load increased. **Figure 17** presents experimental results for the medium-span specimens.

For B-1 and B-2, the failure at the splice was located 12 in. (304.8 mm) below the centerline. For B-3, the failure at the splice was located 36.8 in. (934.7 mm) below the centerline. The failure mechanisms for medium-span specimens were similar to those shown in Fig. 16 (one large crack) but were located at the spliced region.

Table 6 summarizes the capacities from testing the medium-span specimens. Compared with the short-span specimens, the medium-span specimens had fairly low values for capacity and deflection.

Long-span specimens

The long-span slab specimens—C-1, C-2, and C-3—were 219 in. (5563 mm) long by 49 in. (1245 mm) wide by 6 in. (152 mm) thick and had a simply supported span of 215 in.

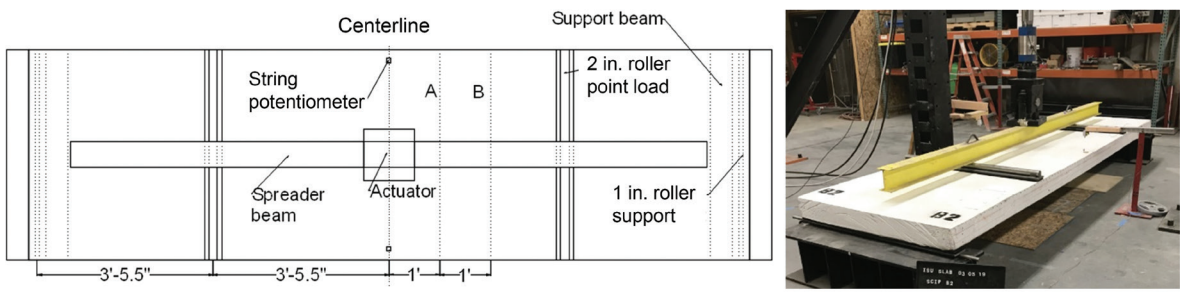

Figure 15. Experimental test setup of the medium-span specimens B-1, B-2, and B-3. Note: A and B denote locations of splice planes. B-1 = specimen B-1; B-2 = specimen B-2; B-3 = specimen B-3. 1" = 1 in. = 25.4 mm; 1' = 1 ft = 0.305 m.

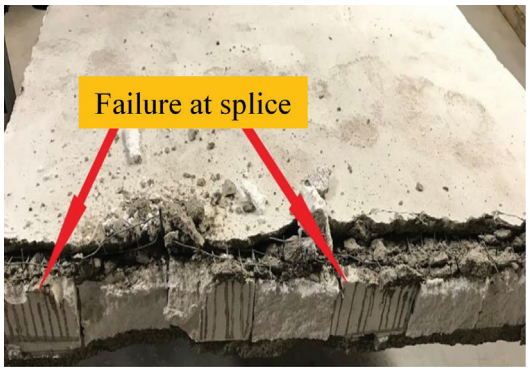

Figure 16. Typical failure plane for the medium-span specimens.

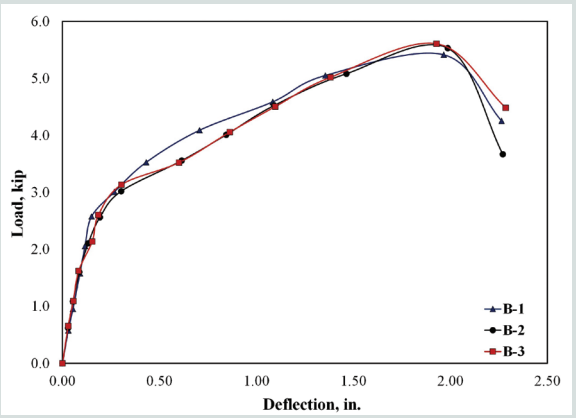

Figure 17. Load-deflection curves for the medium-span specimens. Note: B-1 = specimen B-1; B-2 = specimen B-2; B-3 = specimen B-3. 1 in. = 25.4 mm; 1 kip = 4.448 kN.

Table 6. Summary of test results for medium-span specimens

Specimen	f'_c, psi	k, lb/in.	M_{cr}, kip-ft	M_{max}, kip-ft	δ, in.	W, lb/ft²
B-1	7453	17,158	4484	9419	1.97	95.3
B-2	7160	13,269	4455	9620	1.99	97.3
B-3	7647	14,057	4526	9755	1.93	98.7
Average	7420	14,828	4489	9598	1.96	97

Note: f'_c = compressive strength of concrete at 28 days; k = elastic stiffness; M_{cr} = cracking moment; M_{max} = ultimate moment capacity; W = ultimate uniform load that can produce a similar ultimate moment capacity M_{max}; δ = deflection at ultimate load. 1 in. = 25.4 mm; 1 lb/in. = 0.00018 kN/mm; 1 kip-ft = 1.356 kN-m; 1 psi = 6.895 kPa; 1 lb/ft² = 4.88 kg/m².

(5461 mm). **Figure 18** presents the schematic details and the test setup for the long-span slab specimens.

Similar to the medium-span slabs, the long-span specimens had a splice that was located at the center of the panels without any additional reinforcement. The two splice planes (labeled A and B) can be seen in Fig. 18.

Hairline cracks appeared on the bottom wythe in the critical moment region during load levels of 1 and 1.5 kip (4.44 and 6.66 kN). The behavior of the long-span specimens was similar to that of the medium-span specimens. Shortly after flexural cracks appeared, the specimens yielded. As the load increased, a dominant crack in the splice region became more obvious. Very few cracks were recorded outside of the critical moment region.

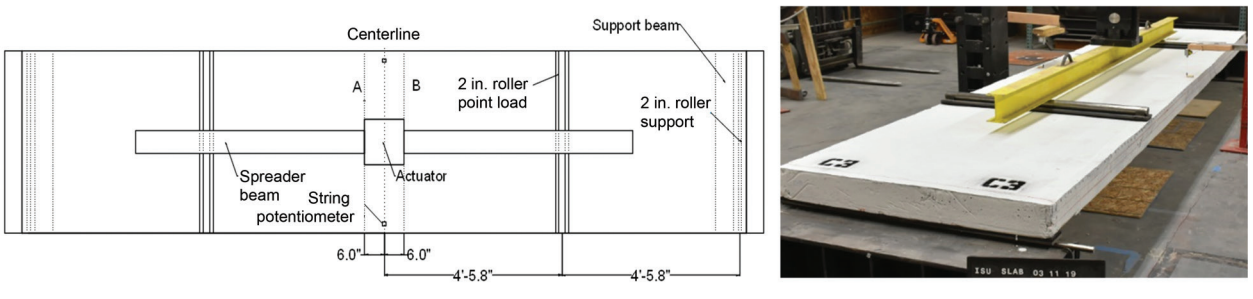

Figure 18. Experimental test setup of the long-span specimens C-1, C-2, and C-3. Note: A and B denote locations of splice planes. C-1 = speciment C-1; C-2 = specimen C-2; C-3 = specimen C-3. 1" = 1 in. = 25.4 mm; 1' = 1 ft = 0.305 m.

The modes of failure for C-1, C-2, and C-3 were identical. The specimens failed prematurely at the splice location under flexural loading. There was little to no stress redistribution and inelastic deformation in testing of the specimens. For C-1 and C-3, failure occurred at the splice location approximately 12 in. (304.8 mm) above the centerline. For C-2, the failure plane was located at a similar distance from the centerline, but failure occurred below the centerline.

Figure 19 presents the experimental results from testing of the long-span specimens. **Table 7** summarizes the testing results. The cracking moment and elastic stiffness of the long-span specimens were considerably lower than for the medium- and short-span samples.

Modified long-span specimens

Two modified long-span specimens with additional reinforcement at the splice location were prepared for experimental testing. The goal was to avoid premature failure in the splice zones for the medium- and long-span specimens. Additional splice reinforcement at the splice region was intended to shift failure outside the splice zones.

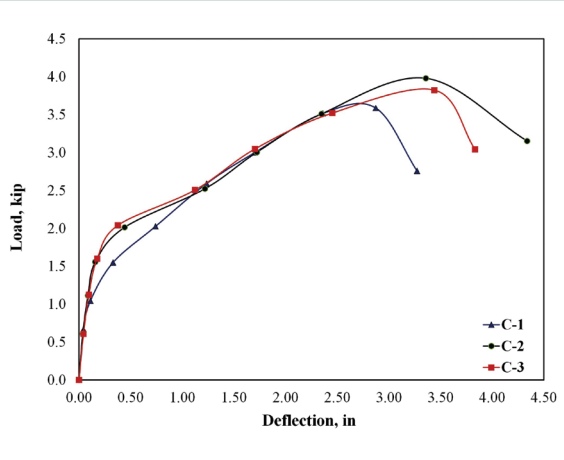

Figure 19. Load-deflection curves for the long-span specimens C-1, C-2, and C-3. Note: C-1 = specimen C-1; C2 = specimen C-2; C-3 = specimen C-3. 1 in. = 25.4 mm; 1 kip = 4.448 kN.

The modified long-span specimens—S-1 and S-2—were 219 in. (5563 mm) long by 49 in. (1245 mm) wide by 6 in. (150 mm) thick and had a simply supported span of 215 in. (5461 mm) (Table 2). The schematic details and the test setup for the modified long-span slab specimen were exactly the same as the long-span specimen shown in Fig. 18. **Figure 20** presents the reinforcement details of the splice region for S-1 and S-2.

S-1 and S-2 had ductile failures dominated by flexural action. The additional reinforcement provided at the splice zones increased the ultimate load-carrying capacity of the specimens by approximately 40%. The deflection at ultimate load was more than 200% that of the long-span specimen without additional reinforcement. There was no premature failure at the splice locations, and the failure planes were shifted away from the splice locations. **Figure 21** presents the load-deflection plots for the modified long-span specimens.

Hairline cracks appeared on the bottom wythe in the critical moment region during load levels of 1.5 and 2 kip (6.66 and 8.88 kN). Many cracks appeared before the specimens started to yield. The number of cracks observed in the testing of S-1 and S-2 were significantly higher than what was observed in the testing of medium- and long-span specimens without additional reinforcement at the splice locations.

For S-1, once yielding occurred, no new cracks were observed and only a few of the existing cracks started to widen. The widening of cracks continued until the dominant cracks appeared and caused failure of the specimen. For S-1, the ultimate failure plane was located where the additional reinforcement ended. The failure occurred 24 in. (609.6 mm) above the centerline (**Fig. 22**).

In the testing of S-2, new cracks appeared after yielding and few of the existing cracks started to widen. The widening continued until two dominant cracks were formed. Because the reinforcing bars in S-2 were staggered, the failure plane was not over a straight line. The failure occurred 12 in. (304.8 mm) above the centerline (Fig. 22). Overall, the configuration used at the splice location for S-1 was more effective than S-2. **Table 8** summarizes the capacities observed during testing of the modified long-span specimens.

Table 7. Summary of test results for the long-span specimens

Specimen	f'_c, psi	k, lb/in.	M_{cr}, kip-ft	M_{max}, kip-ft	δ, in.	W, lb/ft²
C-1	8184	9436	2341	8037	2.87	49.1
C-2	7098	9851	3488	8916	3.36	54.4
C-3	7109	9073	3586	8565	3.44	52.3
Average	7464	9453	3138	8506	3.22	52

Note: f'_c = compressive strength of concrete at 28 days; k = elastic stiffness; M_{cr} = cracking moment; M_{max} = ultimate moment capacity; W = ultimate uniform load that can produce a similar ultimate moment capacity M_{max}; δ = deflection at ultimate load. 1 in. = 25.4 mm; 1 lb/in. = 0.00018 kN/mm; 1 kip-ft = 1.356 kN-m; 1 psi = 6.895 kPa; 1 lb/ft² =4.88 kg/m².

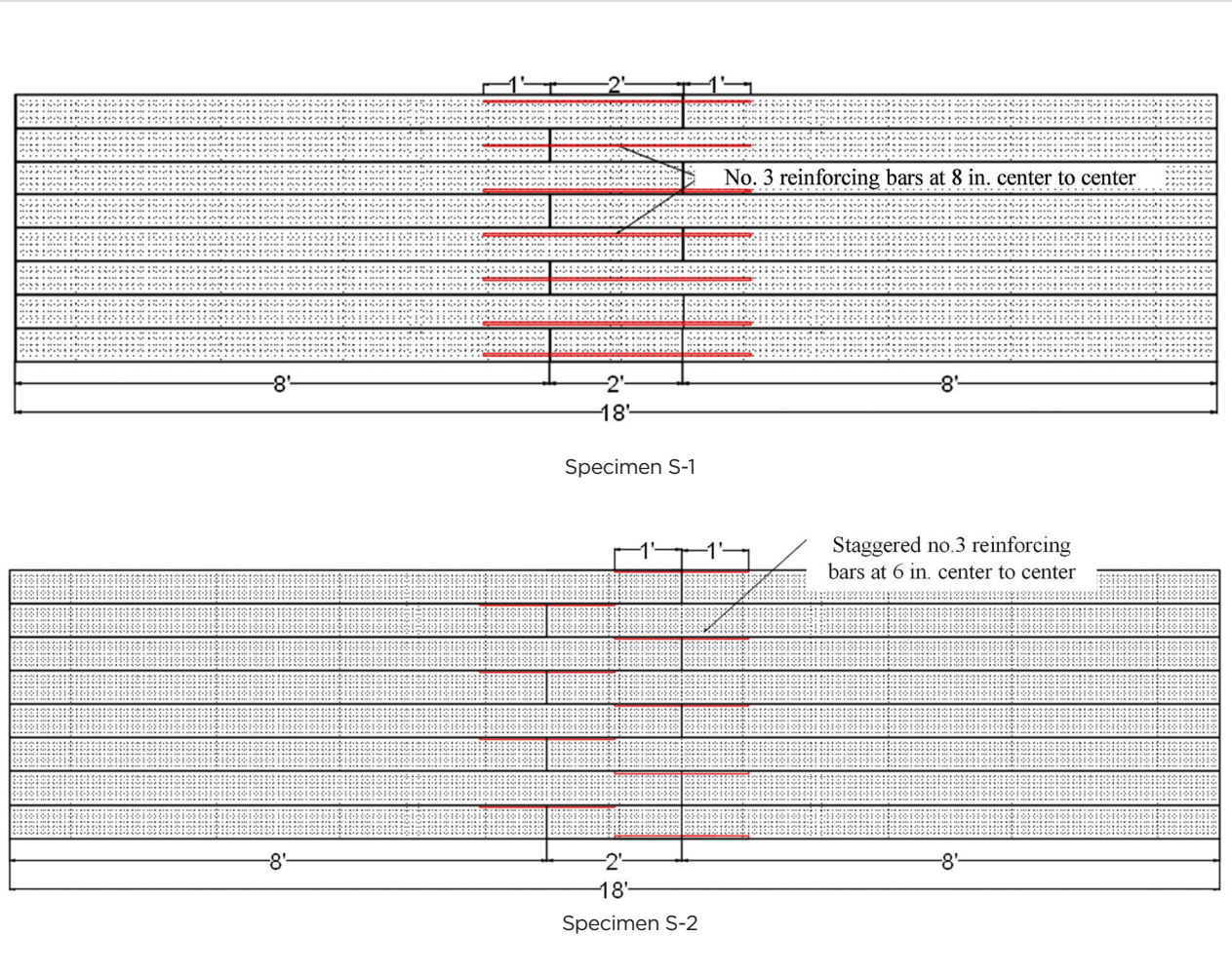

Figure 20. Reinforcing bar details of the splice for the modified long-span specimens. Note: no. 3 = 10M; 1" = 1 in. = 25.4 mm; 1' = 1 ft = 0.305 m.

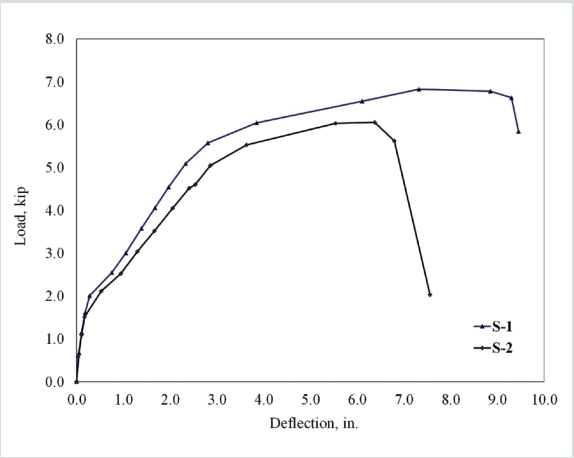

Figure 21. Load-deflection curves for the modified long-span specimens S-1 and S-2. Note: S1 = specimen S-1; S-2 = specimen S-2. 1 in. = 25.4 mm; 1 kip = 4.448 kN.

Discussion

This section discusses ultimate flexural capacities, building code requirements, and composite behavior for SCIPs. The discussion for composite has been developed in accordance with Fouad et al.[10]

Total ultimate moment capacity

To check whether additional reinforcement in the long-span specimens increased the total moment capacity of the slabs, the total moment capacities for each span were calculated. The total moment for each span was calculated as the sum of the moment caused by the self-weight of the slabs and the average applied moments. An average self-weight of 135 lb/ft (1.97 kN/m) was assumed for all spans. **Table 9** and **Fig. 23** present the results for the total moment capacities of the slabs. The average ultimate moment capacity for the short-span specimens was 16.2 kip-ft (22.1 kN-m). Compared with the capacity of the short-span specimens, the total moment capac-

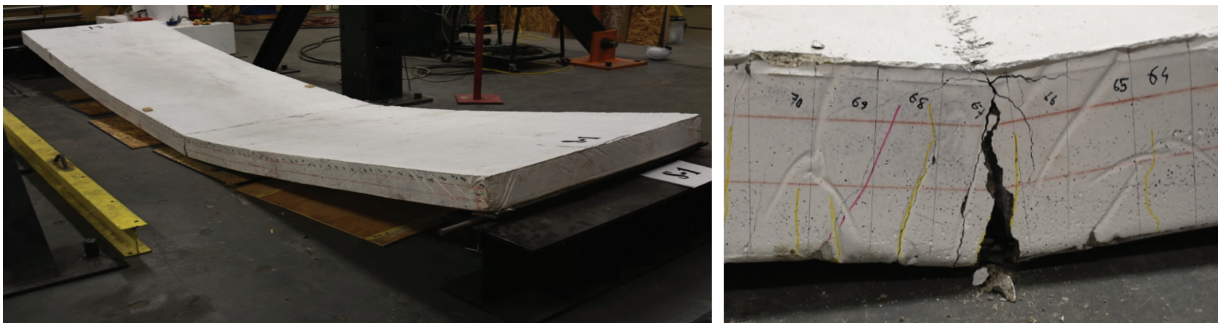

Specimen S-1

Specimen S-2

Figure 22. Failure modes for the modified long-span specimens.

Table 8. Summary of test results for the modified long-span specimens

Specimen	f'_c, psi	k, lb/in.	M_{cr}, kip-ft	M_{max}, kip-ft	δ, in.	W, lb/ft²
S-1	6432	11,344	3612	15,166	8.84	92.6
S-2	7109	10,243	3393	13,541	6.38	82.6
Average	6771	10,793	3502	14,354	7.61	88.0

Note: f'_c = compressive strength of concrete at 28 days; k = elastic stiffness; M_{cr} = cracking moment; M_{max} = ultimate moment capacity; W = ultimate uniform load that can produce a similar ultimate moment capacity M_{max}; δ = deflection at ultimate load. 1 in. = 25.4 mm; 1 lb/in. = 0.00018 kN/mm; 1 kip-ft = 1.356 kN-m; 1 psi = 6.895 kPa; 1 lb/ft² =4.88 kg/m².

Table 9. Summary of average ultimate moment capacities

Specimen	M_d, kip-ft	M_a, kip-ft	M_{tot}, kip-ft
Short span	1.7	16.2	18.0
Medium span	3.3	9.6	12.9
Long span	5.4	8.5	13.9
S-1	5.4	15.2	20.6
S-2	5.4	13.5	18.9

Note: M_a = applied moment during testing; M_d = moment due to self-weight; M_{tot} = total moment capacity. 1 kip-ft = 1.356 kN-m.

ities for the unmodified medium- and long-span specimens were significantly reduced. These reductions in total moment capacity were mainly due to premature failures at the splices. The total moment capacity for the modified long-span specimens was slightly higher than that of the short-span specimens. This result was due to the additional reinforcement that was provided in the modified long-span specimens.

Building code requirements

SCIPs are generally designed for construction of residential structures. Floor or roof slabs made of SCIPs are designed "one way." In this section, some requirements pertinent to U.S. building codes are discussed. According to ASCE 7-16,[23] the minimum uniformly distributed floor live load for a

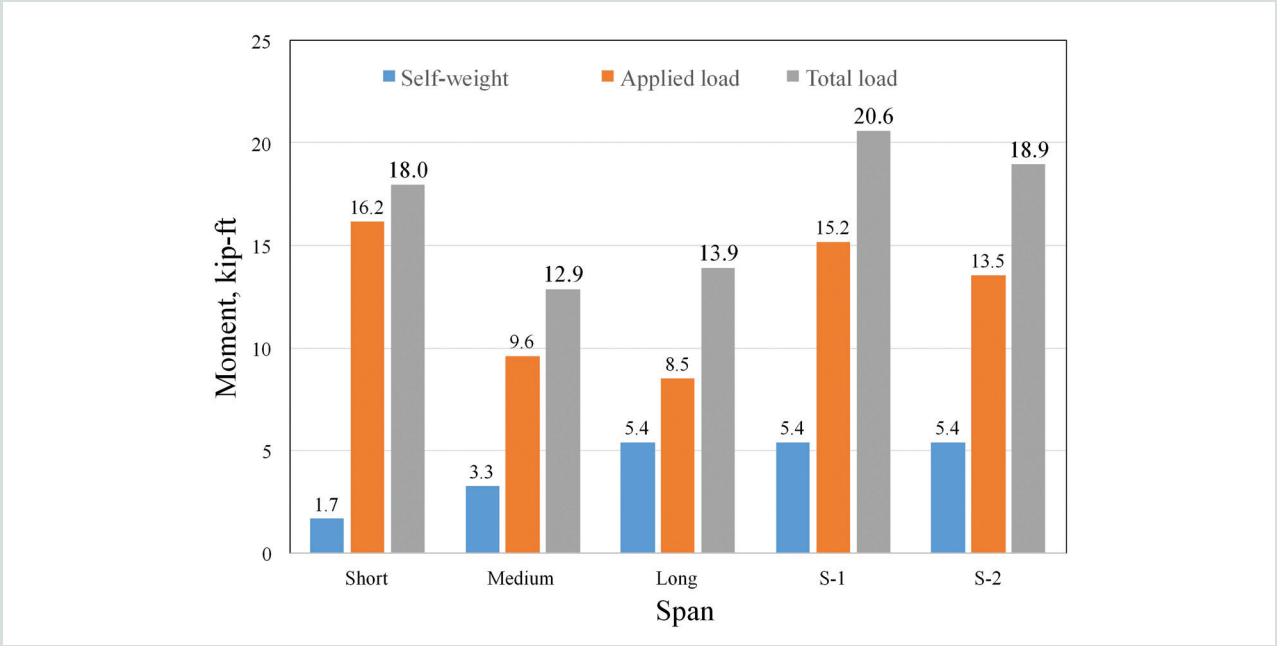

Figure 23. Average ultimate moment capacities for the specimens. Note: S-1 and S-2 are modified long-span specimens. 1 kip-ft = 1.356 kN-m.

residential structure is 40 lb/ft^2 (1.9 kPa). For the roof, the minimum live load is 20 lb/ft^2 (0.96 kPa). With a live load factor of 1.6, these loads are 64 and 32 lb/ft^2 (3.1 and 1.5 kPa) for the floor and roof, respectively. Using simple calculations, an equivalent load from the testing setup conducted in this research can be obtained for the aforementioned minimum live loads dictated by the building code. The maximum permissible deflection for one-way concrete slabs according to ACI 318-19[18] can be taken to be $L/360$ for floors and $L/180$ for roofs of the clear span length. The deflection of the slab δ at a corresponding equivalent load P can be obtained from the experimental data and compared against the maximum permissible value to check whether a specimen satisfies the code requirement for a residential floor or roof slab. **Table 10** summarizes this requirement. For the minimum allowable factored live load, the corresponding average deflection is obtained

Table 10. Summary of the code requirements for one-way slabs

Span length	Specimens	$\delta_{allowable}$, in.		W_u, lb/ft^2	W_L, lb/ft^2		P, kip-ft		$\delta_{allowable} > \delta$	
		Floor ($L/360$)	Roof ($L/180$)		Floor	Roof	Floor	Roof	Floor	Roof
Short	A-1	0.3	0.7	317	64	32	2592	1296	Yes	Yes
	A-2			331.9						
	A-3			325						
Medium	B-1	0.5	0.95	95.3			3637	1818	No	Yes
	B-2			97.3						
	B-3			98.7						
Long	C-1	0.6	1.2	49.1			4682	2341	No	Yes
	C-2			54.4						
	C-3			52.3						
	S-2			82.6						

Note: L = length of the span; W_L = minimum factored live load from ASCE 7-16; W_u = ultimate load carrying capacity; δ = deflection at ultimate load; $\delta_{allowable}$ = maximum permissible deflection from ACI 318-19. 1 lb/ft^2 =4.88 kg/m^2.

for both the roof and floor. Short-span specimens had an average deflection of 0.044 in. (1.12 mm), which was checked against the floor's minimum factored live load W_L (Table 10). The deflection criteria were satisfied for both floor and roof panels. Medium-span specimens had an average deflection of 0.12 in. (3.05 mm), which was checked against the roof minimum factored live load W_L. The deflection criteria for the roof were satisfied, but the specimen had already yielded for floor minimum factored live load W_L. Similarly, long-span specimens had an average deflection of 0.75 in. (19.05 mm), which was checked against the roof minimum factored live load W_L and satisfied the deflection limit; however, at that point, the slabs were already exhibiting cracking. The long-span specimens had already yielded at floor minimum factored live load W_L and did not satisfy the requirement.

In summary, the short-span specimens satisfied the requirements from the building code for applications such as floor and roof slabs. For the medium- and long-span specimens, the slabs satisfied the building code requirements only for application as roof slabs.

Additional flexural reinforcing bars can be used to increase the moment capacity of the specimens, which is a common practice in construction with SCIPs. Similarly, it is important to provide reinforcing bars at the splice locations to prevent premature failures. The thickness of the concrete skin can also be increased to achieve higher cracking moments for the slabs and thus increase flexural strength.

Composite action

Depending on the degree of composite action achieved, a sandwich panel can be divided into three categories: fully composite, partially composite, and noncomposite. A panel is considered to be a fully composite section when 100% of the longitudinal shear is transferred between the two load-bearing faces. On the other hand, if there is no transfer of shear between the two faces, the section is considered to be noncomposite. Last, a panel is considered to be partially composite when the shear connectors transfer only a fraction of the longitudinal shear.[24]

The flexural capacity of short-span SCIPs was analyzed as fully composite and noncomposite sections. The actual flexural capacity of the panels obtained from the experimental program was then used to determine the degree of composite action achieved by the panels.

Flexural calculations, per ACI 318-19,[17] used actual dimensions and details of a short-span slab for the analysis. The clear span of the slab was assumed to be 119 in. (3023 mm), and the slab was assumed to be 49 in. (1.2 m) wide by 6 in. (152 mm) thick. A self-weight of 131 lb/ft (1.91 kN/m) was considered for the panel. Because the experimental test results showed that no short-span specimen had a shear failure at the supports, a minimum shear capacity equal to half of the ultimate load, or 6.6 kip (29.36 kN), was assumed for the panels. The average compressive strength of concrete was assumed to be 8000 psi (55.16 MPa). This assumption was based on the average concrete strength of the panels on testing day. For the hard-drawn mesh and the trusses, the yield strength was conservatively assumed to be 60 ksi (413.7 MPa). The flexural calculations accounted for the area of steel from both the mesh and the trusses (bottom chord).

Although sandwich beam theory was not followed in this research, it is important to consider this theory for further analysis of the composite action. In the sandwich beam theory, the axial strain is assumed to vary linearly over the cross section of the beam, as in the Euler-Bernoulli beam theory. This assumption can then be considered to obtain the important parameters such as flexural rigidity and shear stiffness of the sandwich panels. The possible modes of failure investigated for the SCIP slabs were flexure, shear, and compression. Results and observations from experimental testing of SCIPs with three different spans (10, 14, and 18 ft [3.0, 4.3, and 5.5 m]) showed that the primary mode of failure was flexure for the short-span specimens as well as the medium- and long-span specimens if appropriate splicing details were incorporated.

Fully composite section For this part of the analysis, the specimen was assumed to be a fully composite section. According to section 7 of ACI 318-19,[17] a fully composite slab of concrete elements can be designed for flexure as a solid, reinforced concrete slab but connected so that all elements resist loads as a unit. Hence, for this analysis the cross section of the panels was assumed to be a solid, reinforced concrete slab with two layers of reinforcement. The mesh and the truss chords at the bottom wythe were considered to be the tensile steel, and the reinforcement at the top face was assumed to be the compression steel. The total area of steel in each wythe was calculated to be 0.522 in.^{2} (337 mm^2). The nominal moment capacity ϕM_n was calculated using the effective moment, which is similar to the flexure design of a doubly reinforced concrete slab.

$$\phi M_n = 0.85 f_c' ab\left(d - \frac{a}{2}\right) + A_s' f_s'\left(d - d'\right)$$

where

f_c' = compressive strength of concrete

a = distance to the neutral axis

b = width of the concrete slab

d = distance to tension steel

A_s' = area of compression steel

f_s' = stress in compression bars

d' = distance to compression steel

The analysis shows that the total moment capacity for a fully composite section is expected to be 13.7 kip-ft (18.6 kN-m). The moment caused by the self-weight of the panel can be subtracted to calculate the effective moment capacity. The net effective moment capacity in this instance would be 12.2 kip-ft (16.54 kN-m), which corresponds to an equivalent test load of 9.86 kip (43.86 kN).

Noncomposite section For this part of the analysis, a noncomposite section was assumed for the sandwich panel. For a noncomposite section, there is no transfer of stresses in between the two wythes; therefore, the wythes resist the flexure loads as two individual sections. The cross-section area used for this analysis was similar to that of one individual wythe. Unlike the analysis for a fully composite section, where both the compression and tension steel were used, only one layer of tensile reinforcement was used for this analysis. The following equation was used to calculate the total moment capacity for the noncomposite section.

$$\phi M_n = 0.85 f'_c ab\left(d - \frac{a}{2}\right)$$

The analysis shows that the total moment capacity for the noncomposite section can be expected to be 2.4 kip-ft (3.25 kN-m) for two wythes. Similarly, the net effective moment capacity was calculated to be 0.75 kip-ft (1.0 kN-m), which corresponds to an equivalent test load of 1.09 kip (4.85 kN). It is important to consider that deviations in reinforcement location may result in significant strength reduction. Given potential variability in construction and quality of SCIPs, we recommend a more conservative reduction factor of 0.8 instead of 0.9 until further research becomes available. The specimens in the research showed ductile behavior and signs of failure through cracks, buckling, and failure of the mesh (as heard through a series of popping sounds), and more important, significant deflection.

Partially composite section Results from the ACI flexure analysis, assuming a fully composite section, showed that the panels would have an effective moment capacity of 12.2 kip-ft (16.54 kN-m), which corresponds to an equivalent test load of 9.86 kip (43.86 kN). Similarly, the capacity for the noncomposite section was 0.75 kip-ft (1.0 kN-m), which corresponds to an equivalent experimental load of 1.09 kip (4.85 kN). Test results showed that the average effective moment capacity for the short-span specimens was 8.03 kip-ft (10.86 kN-m), with an equivalent test load of 6.76 kip (30.07 kN).

The average load deflection curve obtained from testing the short-span panels along with the calculated capacity of a fully composite and noncomposite section are illustrated in **Fig. 24**. The green line indicates the average yield force obtained experimentally. The two other solid lines indicate the yield force limit derived using theoretical moment capacity of a fully composite and noncomposite section. This indicates that a slab using the SCIP system can achieve partially composite panels. From the load graph, it can be observed that the capacity of the modular SCIPs fell between the fully composite and the noncomposite capacities. The capacity of the SCIPs was closer to that of the fully composite section than that of a noncomposite section. Hence, the modular SCIPs can be classified as a partially composite section. The graph shows that the average effective moment capacity for the modular SCIPs was 66% of the effective capacity of a fully composite section.

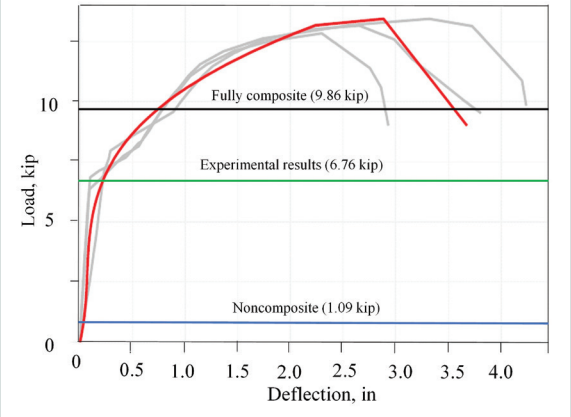

Figure 24. Summary of the composite action of the short-span panels. Note: 1 in. = 25.4 mm; 1 kip = 4.448 kN.

To determine the composite action achieved by the modular SCIPs, the effective moment capacity of the short-span slabs obtained from the experimental program was compared with the capacities of the fully composite and the noncomposite panels that were calculated in the earlier sections.

Conclusion

SCIP construction is an alternative technology for constructing residential homes and low-rise structures. Although there have been various versions of SCIPs developed over the years, this research discusses modular SCIPs that use precasting technology. Eleven full-scale SCIPs with short to long spans were tested under flexural loading. The key conclusions from the research are as follows:

- Results from the four-point bending tests showed good performance of the short-span (10 ft [3 m]) panels. The mode of failure for all three short-span specimens was ductile-flexure-dominated failure when subjected to out-of-plane loading. The panels exhibited substantial nonlinear deformation before failure and achieved 66% effective moment capacity of a fully composite section.
- The short-span specimens satisfied some of the building code criteria for residential concrete floor and roof slabs without additional flexural reinforcement.
- The medium- and long-span specimens, which were 14 and 18 ft (4.3 and 5.5 m) long, respectively, exhibited premature failure at the splice location.

- The splice detail incorporated overlapping wire mesh at the splice region on each skin without additional reinforcement. This detail, which is common in SCIPs, was shown to be inadequate because it prevented the panels from achieving their full capacity.

- Two modified long-span specimens were tested with additional reinforcing bars at the splice region. One configuration used a straight bar pattern, whereas the other used a staggered configuration of additional reinforcing bars at the splice location.

- Testing showed that the capacity and ductility of the long-span panels could be doubled if additional reinforcing bars were incorporated at the splice locations.

- Both splicing configurations were successful in transferring the failure plane away from the splice region and significantly increased the ultimate moment capacity of the panels.

- The straight splicing configuration performed better than other modified long-span configurations. It is recommended that additional flexural reinforcing bars be provided in construction with modular SCIPs.

The thickness of the concrete layer can be increased to provide greater shear and cracking resistance. The overall thickness of the panel can also be increased to achieve higher load capacities.

This study focused on the flexural behavior of modular SCIPs, but further testing is recommended for identifying the axial and shear capacities of this technology.

Acknowledgments

The authors recognize the donation of materials and equipment from Blastcrete Equipment Company. The authors acknowledge the assistance provided by Jared Cantrell and Irene van Woerden with the construction and testing of the specimens and statistical analysis of the data, respectively. Thanks to Rachel Brownell and Jose Duran for proofreading this manuscript.

References

1. Mashal, M., and A. Filiatrault. 2012. "Quantification of Seismic Performance Factors for Buildings Incorporating Three-Dimensional Construction System." Presented at the 15th World Conference on Earthquake Engineering, Lisbon, Portugal. https://www.iitk.ac.in/nicee/wcee/article/WCEE2012_1693.pdf.

2. ASTM International. 2016. *Standard Test Method for Flexural Strength of Concrete (Using Simple Beam with Third-Point Loading).* ASTM C78/C78M-16. West Conshohocken, PA: ASTM International. https://doi.org/10.1520/C0078_C0078M-16.

3. ASTM International. 2018. *Standard Specification for Carbon-Steel Wire and Welded Wire Reinforcement, Plain and Deformed, for Concrete*. ASTM A1064/A1064M-18a. West Conshohocken, PA: ASTM International.

4. ASTM International. 2011. *Standard Specification for Steel Wire for Masonry Joint Reinforcement*. ASTM A951/A951M-11. West Conshohocken, PA: ASTM International. https://doi.org/10.1520/A0951_A0951M-11.

5. ASTM International. 2019. *Standard Specification for Zinc–Coated (Galvanized) Carbon Steel Wire*. ASTM A641/A641M-19. West Conshohocken, PA: ASTM International. https://doi.org/10.1520/A0641_A0641M-19.

6. Mashal, M. 2011. "Quantification of Building Seismic Performance Factors for Building Incorporating Three-Dimensional Construction System." Master of Science thesis, University at Buffalo–State University of New York.

7. Kabir, M. Z. 2005. "Structural Performance of 3-D Sandwich Panels Under Shear and Flexural Loading." *Scientia Iranica* 12 (4): 402–408. http://scientiairanica.sharif.edu/article_2509.html.

8. Matz, K., J. Kügerl, and C. Peheim. 2005. *Structural Engineering Handbook*. Graz, Austria: EVG 3D Construction System.

9. Kabir, M. Z., A. R. Rahai, and Y. Nassira. 2006. "Non-linear Response of Combined System, 3D Wall Panels and Bending Steel Frame Subjected to Seismic Loading." *WIT Transactions on the Built Environment* 85. https://www.witpress.com/elibrary/wit-transactions-on-the-built-environment/85/15956.

10. Fouad, F. H., J. Farrell, M. Heath, A. Shalaby, and A. Vichare. 2009. "The Behavior of the MR Sandwich Panel in Flexure." Special publication 260-06: 73–88. Farmington Hills, MI: ACI.

11. Rezaifar, O., M. Z. Kabir, M. Taribakhsh, and A. Tehranian. 2008. "Dynamic Behaviour of 3D-Panel Single-Storey System Using Shaking Table Testing." *Engineering Structures* 30 (2): 318–337. https://doi.org/10.1016/J.ENGSTRUCT.2007.03.019.

12. Rezaifar, O., M. Z. Kabir, and A. Bakhshi. 2009. "Shaking Table Test of a 1: 2.35 Scale 4-Story Building Constructed with a 3D Panel System." *Scientia Iranica* 16 (3): 199–215. http://scientiairanica.sharif.edu/article_3108.html.

13. El Demerdash, I. M. 2013. "Structural Evaluation of Sustainable Orthotropic Three-Dimensional Sandwich Panel System." PhD diss., University of California, Irvine.

14. Joseph, J., J. Prabakar, and P. Alagusundaramoorthy. 2019. "Insulated Precast Concrete Sandwich Panels under Punching and Bending." *PCI Journal* 64 (2): 68–79. https://doi.org/10.15554/pcij64.2-01.

15. Gurung, K. 2019. "Experimental Investigations of Full-Scale MetRock Structural Concrete Insulated Panels (SCIPs)." Master's thesis, Idaho State University, Pocatello.

16. Mashal, M., K. Gurung, and M. Acharya. 2020. "Full-Scale Experimental Testing of Structural Concrete Insulated Panels (SCIPs)." In *IABSE Congress: Resilient Technologies for Sustainable Infrastructure, Christchurch, New Zealand*, edited by A. Abu, 833–840. Zurich, Switzerland: International Association for Bridge and Structural Engineering. http://dx.doi.org/10.2749/christchurch.2021.0833.

17. ACI. 2019. *Building Code Requirements for Structural Concrete (ACI 318-19) and Commentary (ACI 318R-19)*. Farmington Hills, MI: ACI.

18. ACI. 1991. *Standard Practice for Selecting Proportions for Normal, Heavyweight, and Mass Concrete*. ACI 211.1-91. Farmington Hills, MI: ACI.

19. ASTM International. 2014. *Standard Test Methods for Tension Testing of Metallic Materials*. ASTM E8/E8M. West Conshohocken, PA: ASTM International.

20. ASTM International. 2020. *Standard Test Method for Compressive Strength of Cylindrical Concrete Specimens*. ASTM C39/C39-M. West Conshohocken, PA: ASTM International. https://doi.org/10.1520/C0039_C0039M-20.

21. ASTM International. 2017. *Standard Test Method for Splitting Tensile Strength of Cylindrical Concrete Specimens*. ASTM C496/C496-M. West Conshohocken, PA: ASTM International. https://doi.org/10.1520/C0496_C0496M-17.

22. ASTM International. 2015. *Standard Test Methods of Conducting Strength Tests of Panels for Building Construction*. ASTM E72-15. West Conshohocken, PA: ASTM International. https://doi.org/10.1520/E0072-15.

23. ASCE (American Society of Civil Engineers). 2016. *Minimum Design Loads and Associated Criteria for Buildings and Other Structures*. ASCE7-16. Reston, VA: ASCE.

24. Naji, B., and E. A. Toubia. 2015. "Flexural Analysis and Composite Behavior of Precast Concrete Sandwich Panel." In *Concrete—Innovation and Design: fib Symposium Proceedings*, edited by H. Stang and M. Braestrup, 480–481. Lausanne, Switzerland: *fib* (International Federation for Structural Concrete).

Notation

a = distance to the neutral axis

b = width of the concrete slab

A_s = area of tensile steel

A_s' = area of compression steel

d = distance to tension steel

d' = distance to compression steel

f_c' = compressive strength of concrete

f_s' = stress in compression bars

f_y = yield strength for steel

k = elastic stiffness

L = length or span of the slab

L_d = development length

M_a = applied moment during testing

M_{cr} = cracking moment

M_d = moment due to self-weight

M_{max} = ultimate moment capacity

M_{tot} = total moment capacity

P = equivalent load

W = ultimate uniform load that can produce a similar ultimate moment capacity M_{max}

W_L = minimum live load

δ = deflection of the slab at ultimate load

$\delta_{allowable}$ = maximum permissible deflection

ϕM_n = design moment capacity

About the authors

Mahesh Acharya, EI, is a PhD student in the Department of Civil and Environmental Engineering at Idaho State University in Pocatello. He has a master of science degree in structural engineering from Idaho State University and is a PCI student member.

Karma Gurung, EI, is a structural engineer with Forterra Structural Precast in Salt Lake City, Utah. Gurung has a master of science degree in structural engineering from Idaho State University and is a PCI member.

Mustafa Mashal, PhD, PE, CPEng, IntPE(NZ), is an associate professor in the Department of Civil and Environmental Engineering at Idaho State University. Mashal obtained his PhD from the University of Canterbury in New Zealand. He is a member of several committees for PCI, the American Society of Civil Engineers, the American Concrete Institute, and the Transportation Research Board.

Abstract

Structural concrete insulated panels (SCIPs) are an alternative construction technology to traditional wood framing and masonry units for use in residential homes and low-rise structures. SCIPs can be used to erect structurally sound buildings that are economical, energy efficient, and durable while incorporating sandwich technology. This study presents a novel type of SCIP that can be fabricated using off-the-shelf components. A precasting technology for such modular SCIPs is proposed. Full-scale experimental testing of one-way SCIP slabs with three different span lengths (short, medium, and long) was carried out to investigate flexural behavior, strength, ductility, and failure mechanisms. Testing showed good performance of modular SCIPs under gravity loads. Appropriate splicing details for longer-span SCIPs are developed and tested. Results show that the SCIPs tested in this research can provide a moment capacity equal to 66% of the capacity of a fully composite section.

Keywords

Flexure test, large-scale testing, new technology, self-consolidating concrete, structural concrete insulated panel.

Review policy

This paper was reviewed in accordance with the Precast/Prestressed Concrete Institute's peer-review process. The Precast/Prestressed Concrete Institute is not responsible for statements made by authors of papers in *PCI Journal*. No payment is offered.

Publishing details

This paper appears in *PCI Journal* (ISSN 0887-9672) V. 67, No. 2, March–April 2022, and can be found at https://doi.org/10.15554/pcij67.2-03. *PCI Journal* is published bimonthly by the Precast/Prestressed Concrete Institute, 8770 W. Bryn Mawr Ave., Suite 1150, Chicago, IL 60631.

Reader comments

Please address any reader comments to *PCI Journal* editor-in-chief Tom Klemens at tklemens@pci.org or Precast/Prestressed Concrete Institute, c/o *PCI Journal*, 8770 W. Bryn Mawr Ave., Suite 1150, Chicago, IL 60631.